Device-Level Equivalence and Consistency of Interfacial Dipoles

Yu Wang[1], Feng GAO[1]
1. Department of Physics, Chemistry and Biology (IFM), Linköping University, Linköping 58183, Sweden

Abstract

Interfacial dipoles are commonly represented in semiconductor device models by effective work-function or energy-level shifts. Here, we examine the device-level equivalence of this reduced description by explicitly resolving an interfacial dipole as two oppositely charged spatial regions in a one-dimensional drift–diffusion model. The potential step of the isolated charge double layer is first established analytically and verified numerically. When the same fixed-charge configuration is embedded in different dielectric environments, markedly different potential steps and device responses are obtained, demonstrating that dipole placement must be specified before an equivalent energy-level description can be defined. For a fixed placement, a reduced ETL conduction-band shift reproduces the qualitative carrier redistribution induced by the explicit dipole, but not its magnitude, resulting in different recombination responses and fill-factor losses. We further compare dipole configurations with identical sheet charge density or identical dipole moment. Configurations preserving the dipole moment show substantially closer device responses, although strict equivalence is not achieved. These results identify the dipole moment as an appropriate primary electrostatic descriptor while showing that spatial placement and charge distribution remain significant for the simplification of device-level equivalence.
Keywords: interfacial dipole; space charge; energy-level alignment; carrier redistribution; semiconductor interfaces

1.Introduction

Interfacial dipoles provide a simple means of modifying the electrostatic landscape at semiconductor contacts.[1–3] In device modeling, their effect is therefore often reduced to an equivalent shift of the electrode work function or an effective shift of the relevant energy levels of an adjacent layer[1,4,5]. Such a treatment is intuitive: an isolated dipole produces a potential step, and if only the energy alignment on either side of the interface is of interest, replacing the dipole by the corresponding shift appears sufficient[1,2].

This reduction, however, removes the spatial charge distribution that generates the potential step. In a drift–diffusion device, these fixed charges coexist with mobile carriers and contribute directly to the self-consistent solution of Poisson's equation[1,6,7]. The dipole is therefore not only characterized by an energy-level displacement, but also a spatially resolved electrostatic object whose effect may depend on where its charge is located, the dielectric environment in which it is embedded, and the response of the surrounding semiconductor[1,8,9]. In particular, the same fixed-charge distribution need not generate the same potential step when different parts of the dipole occupy materials with different permittivities. Whether a spatially resolved dipole can be represented by a prescribed energy-level shift at the device level is consequently not obvious.

In this work, we explicitly represent an interfacial dipole as a pair of oppositely charged regions and examine its device-level equivalence using a simplified solar-cell structure as a test system. The electrostatics of the isolated dipole are first established analytically and numerically, providing a well-defined potential step against which reduced descriptions can be compared. We then examine how the spatial placement of the dipole determines the potential step established in the device, and under a fixed placement, to what extent a reduced band-edge shift reproduces the response of the explicit dipole. We further test the consistency of different internal charge configurations by comparing dipoles with the same sheet charge density or the same dipole moment. The aim is to clarify which information is preserved when an interfacial dipole is reduced to a simplified energy-level description, and which aspects require its spatial charge distribution to be retained.

2.Model and Electrostatic Verification

In our primary model, the interfacial dipole is represented as two oppositely and uniformly charged regions with equal thickness d_0, separated by a distance d_1, and carrying fixed charge densities of $+en_0$ and $-en_0$, respectively. For an isolated

dipole embedded in a homogeneous medium with dielectric permittivity ε, integration of Poisson's equation gives the potential difference across the charge double layer as:

$$\Delta \phi_0 = e\frac{n_0 d_0 (d_0 + d_1)}{\epsilon}$$

This dependence on dipole moment per unit area and dielectric environment is consistent with the electrostatics of extended dipolar layers.[1]

The corresponding sheet charge density is ($\sigma = n_0 d_0$), whereas the potential step is determined by both the sheet charge and the separation between the charge centers. Consequently, configurations only with the same σ do not necessarily possess the same dipole moment or potential step because the charge-center separation d_0+d_1 also contributes to the dipole moment. The geometry and charge distribution are illustrated schematically in Fig. 1(a).

The analytical electrostatics were first verified by solving the one-dimensional Poisson equation in COMSOL Multiphysics 6.2. Figure 1b compares simulated electrostatic-potential and electric-field profiles with the analytical solution. Figure 1c further tests the predicted dependence of the potential step on n_0, d_0, and d_1. The numerical results reproduce the expected potential step and field distribution, thereby validating the spatial-charge representation used in the subsequent device calculations.

The dipole model was then incorporated into a one-dimensional drift–diffusion double heterojunction solar-cell structure consisting of a hole transport layer (HTL), absorber, and electron transport layer (ETL). Carrier transport and electrostatics were solved self-consistently using the Semiconductor Module, which solves Poisson's equation together with the drift–diffusion equations for electrons and holes, including Shockley–Read–Hall (SRH), radiative, and Auger recombination.[10] The charged regions were implemented as semiconductor subdomains containing an additional fixed space-charge density, allowing mobile electrons and holes to redistribute self-consistently within and around the dipole region. Zero band offsets were used in the reference structure to isolate the electrostatic effect of the interfacial modification from material-specific energetic barriers. The perovskite (PVSK) is selected owing to their outstanding optoelectronic performance and unique dielectric features.

For comparison, a reduced band-shift model was constructed using the potential step obtained from the isolated dipole. In this representation, the conduction-band edge of the ETL was shifted by the corresponding energy while the explicit space-charge double layer was removed. Only the ETL conduction-band edge was retained in the reduced description because electron transport dominates in the ETL, whereas the hole population remains negligible over the operating range considered. The explicit and reduced descriptions therefore share the same nominal interfacial energy modification but differ in whether the underlying spatial charge distribution is retained. The principal device parameters used in the calculations are summarized in Appendices.

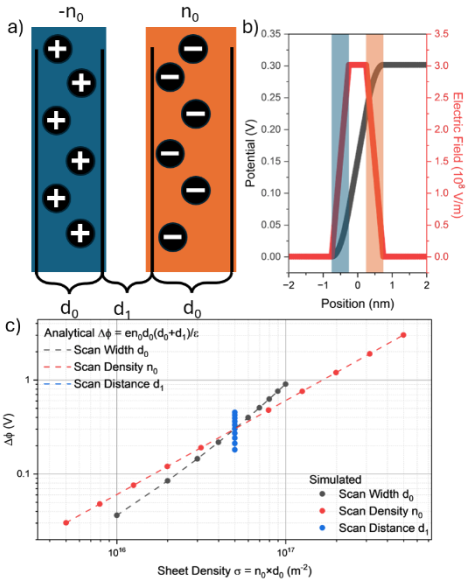


Figure 1. Electrostatic model and verification of the explicit dipole.
(a) Schematic of the spatial charge double layer consisting of two oppositely charged regions of thickness d_0, separated by d_1, with fixed charge densities $\pm en_0$. (b) Simulated electrostatic potential and electric-field profiles compared with the analytical solution for the reference configuration. (c) Dependence of the dipole potential step on n_0, d_0, and d_1, compared with the analytical relation $\Delta\phi_0 = en_0d_0(d_0+d_1)/\varepsilon$.

3.Device-Level Equivalence of Interfacial Dipoles

After establishing the electrostatic behavior of the isolated dipole, we next examine its equivalence under the device operating conditions. Particular attention is given to how the spatial placement of the same nominal dipole affects its device-level electrostatic response, and whether a reduced energy-level description can reproduce the response of the spatially resolved charge distribution. Finally, after fixing the dipole placement, we examine whether different internal charge configurations that preserve the same macroscopic dipole descriptor remain equivalent at the device level.

3.1 Dependence on Dipole Placement

The comparison between an explicit dipole and a reduced band-shift description first requires the spatial placement of the explicit dipole to be

defined. To examine this effect, the same fixed-charge configuration, calculated to produce a 0.3 V potential step when fully embedded in the ETL, was placed entirely in the ETL, equally across the ETL/absorber interface, or entirely in the absorber as shown in Fig.1c.

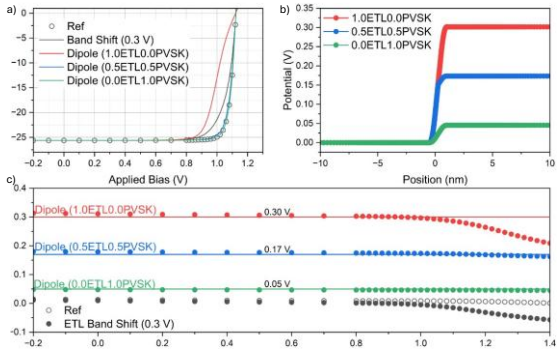


Figure 2. Effect of dipole placement on the device-level response.
(a) Current–voltage characteristics of the reference device, the 0.3 eV ETL band-shift model, and the explicit dipole placed entirely in the ETL, across the ETL/absorber interface, or entirely in the absorber. (b) Standalone electrostatic potential profiles of the same fixed-charge dipole in the three dielectric placements. (c) Potential difference evaluated between the two outer boundaries of the nominal dipole region as a function of applied voltage in the complete device. The different placements generate different local potential differences despite using the same fixed-charge configuration.

As shown in Fig. 2(a), the three placements lead to markedly different current–voltage characteristics. The dipole embedded entirely in the ETL produces the largest deviation from the reference device, whereas the response approaches the reference curve as an increasing fraction of the dipole is moved into the absorber. The device response therefore exhibits a pronounced dependence on dipole placement.

The origin of this is revealed by the electrostatic analysis in Fig. 2(b). For the same fixed-charge distribution, the potential difference established across the dipole region decreases from approximately 0.30 V for the ETL-embedded configuration to 0.17 V for the interfacial configuration and 0.05 V when the dipole is placed entirely in the absorber. This variation arises from the different dielectric environments sampled by the spatially distributed charges, since the potential generated by a charge double layer depends on the dielectric permittivity of the surrounding medium. Although the dielectric environment changes the electrostatic potential step associated with the same fixed-charge configuration, Figure 2(c) further shows that these differences still persist under applied bias. At higher forward bias, the extracted local potential difference becomes increasingly bias dependent as the device-level electrostatic potential is superimposed on the fixed dipolar contribution.

These results show that a fixed-charge dipole cannot be assigned a unique device-level potential step without specifying the dielectric environment in which it is embedded. In the following comparisons, the dipole is therefore placed entirely within the ETL, for which the potential difference across the explicit dipole remains close to the standalone value of 0.3 V over the relevant operating range. This configuration provides a well-defined basis for comparison with the corresponding reduced band-shift description.

3.2 Comparison with the Band-Shift Approximation

With the dipole fixed entirely within the ETL, the explicit model was compared with a reduced description in which the ETL conduction-band edge was shifted by 0.3 eV. As shown in Fig. 2a, both treatments modify the J–V characteristic in the same qualitative direction, but with different magnitudes: the explicit dipole causes a larger reduction in fill factor, while the short-circuit current and open-circuit voltage remain nearly unchanged. This suggests that the reduced band-shift description captures the overall tendency of the interfacial modification, while its quantitative effect under finite forward bias differs from that of the explicit dipole.

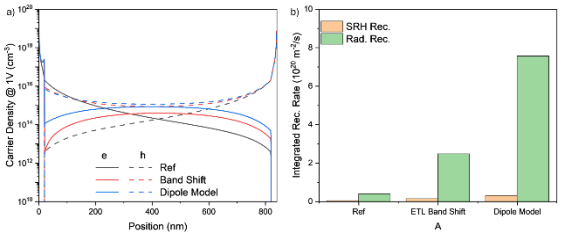


Figure 3. Carrier redistribution and recombination induced by the interfacial modification.
(a) Electron and hole concentration profiles at an applied voltage of 1 V for the reference, ETL conduction-band-shift, and explicit-dipole models. Both interfacial treatments produce qualitatively similar carrier redistribution, with a larger magnitude in the explicit-dipole model. (b) Corresponding radiative and Shockley–Read–Hall (SRH) recombination contributions. The enhanced carrier overlap is accompanied primarily by an increase in radiative recombination, whereas the SRH contribution changes only slightly.

Figure 3 compares the carrier distributions at an applied voltage of 1 V, within the forward-bias range where the J–V responses of the three models are clearly distinguishable. Relative to the reference device, both the band-shift and explicit-dipole models redistribute electrons and holes in the same general direction, showing that the reduced band-shift description reproduces the direction of the carrier redistribution induced by the explicit dipole. The redistribution is, however, substantially stronger in the explicit model, leading to greater

spatial overlap of the electron and hole populations within the absorber.

This difference is reflected in the recombination responses. The increased carrier overlap is accompanied by a pronounced increase in radiative recombination, whereas the change in SRH recombination is comparatively small. The stronger redistribution and recombination in the explicit-dipole model are therefore consistent with the larger current loss observed in the fill-factor region. Thus, the reduced band shift provides a useful qualitative representation of the dipole-induced device response, but does not quantitatively reproduce its magnitude] under operating conditions.

3.3 Consistency of Different Dipole Configurations

The explicit dipole model also allows the internal charge configuration to be varied while preserving selected macroscopic quantities. Two sets of configurations were considered by changing n_0 and d_0 while keeping the dipole placement and d_1 fixed. In the first set, the sheet charge density, $\sigma=n_0d_0$, was kept constant. In the second set, the dipole moment per unit area, proportional to $n_0d_0(d_0+ d_1)$, was kept constant, corresponding to the same standalone potential step which, for the fixed dielectric environment considered here, also preserves the standalone potential step.

As shown in Fig. 4(a), configurations with the same sheet charge density produce noticeably different J–V characteristics. This is consistent with the analytical electrostatics, since a constant σ does not preserve the separation-weighted dipole moment and therefore does not correspond to the same potential step. Sheet charge density alone is therefore insufficient to establish electrostatic equivalence between different spatial realizations of the dipole.

A substantially better collapse agreement between the J–V characteristics is obtained when the dipole moment is held constant, as shown in Fig. 4(b). The resulting J–V curves remain close to one another, indicating that the dipole moment is a more appropriate descriptor of device-level equivalence than the sheet charge density alone. Small residual differences nevertheless remain, showing that identical standalone dipole moments do not lead to strictly identical operating characteristics.

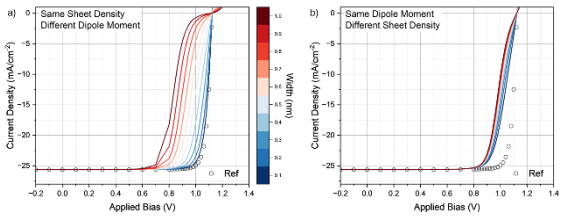


Figure 4. Device-level consistency of different explicit dipole configurations.
Current–voltage characteristics for dipole configurations with different n_0 and d_0 while maintaining (a) the same sheet charge density, $\sigma= n_0d_0$, and (b) the same dipole moment, proportional to $n_0d_0(d_0+d_1)$. The reference-device J–V characteristic is shown as a solid line for comparison. Configurations with equal dipole moment exhibit substantially closer device responses than those with equal sheet charge density, although complete equivalence is not obtained.

These results indicate that the dipole moment provides a more appropriate electrostatic description for comparing different spatial realizations of the dipole, while the detailed charge distribution remains relevant to the self-consistent device response. Thus, device-level equivalence becomes substantially improved, but remains approximate, even when the standalone potential step is preserved.

4. Discussion

The results highlight a distinction between the potential step associated with an interfacial dipole and its complete device-level response. For a fixed dielectric environment, the electrostatics of the isolated dipole are well described by its dipole moment per unit area, and configurations preserving this quantity exhibit substantially better device-level consistency than those preserving the sheet charge density alone. The dielectric environment must, however, be specified together with the charge configuration, since the same fixed-charge double layer can generate different potential steps when embedded in materials with different permittivities[1].

Once the dipole is embedded in the complete device, its fixed charge acts together with the mobile semiconductor space charge in the self-consistent electrostatic and transport solution. Importantly, the potential step associated with the fixed dipole remains essentially preserved for the ETL-embedded configurations considered here; the residual differences between configurations with equal dipole moment therefore arise from their different spatial charge distributions and the corresponding self-consistent carrier response. Equal dipole moments, or equal standalone potential steps, can consequently yield closely similar but not strictly identical current–voltage characteristics.

The comparison with the reduced band-shift description provides a complementary view of this distinction. The prescribed conduction-band shift reproduces the qualitative direction of the carrier redistribution induced by the explicit dipole, indicating that the energy-level picture captures the principal trend observed in the device response. The explicit model, however, retains the finite spatial

distribution of the fixed charges and in the present calculations produces a different magnitude of carrier redistribution and recombination under operating bias. The approximation should therefore be regarded as a reduced device description rather than a quantitatively equivalent representation of the underlying dipolar charge distribution.

The present model intentionally isolates these electrostatic effects. The transport layers and absorber were assigned idealized band alignment, and the dipole regions were treated as semiconductor domains containing additional fixed charge while remaining accessible to mobile carriers. This representation is not intended to reproduce the microscopic electronic structure of a particular molecular or interfacial layer. Real interfacial dipoles can additionally involve chemical bonding, charge transfer, molecular polarization, and other microscopic interfacial processes that are not resolved in the present continuum description.[2] Instead, the present construction provides a controlled means of separating the electrostatic consequences of a spatially resolved charge double layer from material-specific interfacial effects. The conclusions should therefore be interpreted in the context of classical drift–diffusion descriptions of semiconductor interfaces, rather than as a microscopic model of a specific material combination.

5. Conclusions

The present results show that the device-level description of an interfacial dipole cannot be reduced unconditionally to a single energy-level shift. For an isolated charge double layer in a fixed dielectric environment, the potential step is governed by the dipole moment per unit area, providing a natural electrostatic descriptor. Once the same charge distribution is embedded in a device, however, its effective electrostatic action also depends on where it is placed, because different dielectric environments modify the potential established by the dipole.

When the placement is fixed, such that the explicit dipole retains the intended potential step, a reduced band shift reproduces the qualitative direction of the carrier redistribution, but not its full magnitude. The resulting differences in carrier overlap and recombination are reflected primarily in the fill-factor region of the J–V characteristic. The reduced energy-level picture is therefore physically meaningful as a first-order description, but it is not quantitatively equivalent to the spatially resolved dipole under operating conditions.

The same distinction appears when different internal realizations of the explicit dipole are compared. Preserving the sheet charge density alone does not ensure electrostatic or device-level equivalence, whereas preserving the dipole moment leads to much closer J–V characteristics. The remaining differences indicate that even an identical standalone potential step does not uniquely determine the complete device response. In an operating semiconductor device, the fixed dipolar charge distribution and the self-consistent mobile space charge must be considered together.

Interfacial dipoles can therefore be described by an effective potential step only within a clearly defined dielectric and device environment. The dipole moment provides the appropriate first-order electrostatic descriptor, while spatial placement and charge distribution determine the limits of its device-level equivalence.

Reference

1. Zojer, E., Taucher, T. C. & Hofmann, O. T. The Impact of Dipolar Layers on the Electronic Properties of Organic/Inorganic Hybrid Interfaces. *Adv. Mater. Interfaces* **6**, 1900581 (2019).
2. Chen, Q., Wang, C., Li, Y. & Chen, L. Interfacial Dipole in Organic and Perovskite Solar Cells. *J. Am. Chem. Soc.* **142**, 18281–18292 (2020).
3. Ma, Y., Gong, J., Zeng, P. & Liu, M. Recent Progress in Interfacial Dipole Engineering for Perovskite Solar Cells. *Nano-Micro Lett.* **15**, 173 (2023).
4. Lin, W. M. M. *et al.* Recombination Dynamics in PbS Nanocrystal Quantum Dot Solar Cells Studied through Drift–Diffusion Simulations. *ACS Appl. Electron. Mater.* **3**, 4977–4989 (2021).
5. Mazzarella, L. *et al.* Strategy to mitigate the dipole interfacial states in (i)a-Si:H/MoOx passivating contacts solar cells. *Prog. Photovolt. Res. Appl.* **29**, 391–400 (2021).
6. Calado, P. *et al.* Driftfusion: an open source code for simulating ordered semiconductor devices with mixed ionic-electronic conducting materials in one dimension. *J. Comput. Electron.* **21**, 960–991 (2022).
7. Zojer, K. Simulation of Charge Carriers in Organic Electronic Devices: Methods with their Fundamentals and Applications. *Adv. Opt. Mater.* **9**, 2100219 (2021).
8. Vilan, A. & Cahen, D. Chemical Modification of Semiconductor Surfaces for Molecular Electronics. *Chem. Rev.* **117**, 4624–4666 (2017).
9. Lambrecht, W. R. L. & Segall, B. Interface-bond-polarity model for semiconductor heterojunction band offsets. *Phys. Rev. B* **41**, 2832–2848 (1990).
10. *Semiconductor Module User's Guide, COMSOL Multiphysics 6.2*. (COMSOL AB, 2023).

Acknowledgement

We would like to acknowledge the financial support from the European Research Council (LEAP, No. 101045098). F.G. is a Wallenberg Scholar.

Data availability

All data supporting the findings of this study are available within the article. Source data are available via Zenodo at https://doi.org/10.5281/zenodo.23051064.

Appendix

Appendix 1 Parameters for Default Device Configuration of Transport Layers

Name	Unit	Value
ETL Thickness	nm	20
HTL Thickness	nm	20
ETL Permittivity	1	3
HTL Permittivity	1	3
Band Offset ETL/Absorber	V	0.0
Band Offset ETL/Absorber	V	0.0
mun_ETL	cm^2/V/s	1e-3
mup_ETL	cm^2/V/s	1e-7
mun_HTL	cm^2/V/s	1e-7
mup_HTL	cm^2/V/s	1e-3
Nd_ETL	cm^-3	1e17
Na_HTL	cm^-3	1e17

Appendix 2 Parameters for Default Device Configuration of Absorber

Name	Unit	Value
Absorber Thickness	nm	800
Absorber Permittivity	1	20
mun_Absorber	cm^2/V/s	1
mup_Absorber	cm^2/V/s	1
Nd_Absorber	cm^-3	1e13
SRH Lifetime	s	1e-5
Rad Coefficient	cm^3/s	1e-9
Auger Coefficient	cm^6/s	1e-28
Generation Rate	cm^-3/s	2e21